

Results of the 1993 NASA/JPL Balloon Flight Solar Cell Calibration Program

B. E. Anspaugh
R. S. Weiss

N94-24563

Unclass

G3/44 0206657

October 1, 1993



National Aeronautics and
Space Administration

Jet Propulsion Laboratory
California Institute of Technology
Pasadena, California

(NASA-CR-195158) RESULTS OF THE
1993 NASA/JPL BALLOON FLIGHT SOLAR
CELL CALIBRATION PROGRAM (JPL)
23 p

JPL Publication 93-30

Results of the 1993 NASA/JPL Balloon Flight Solar Cell Calibration Program

B. E. Anspaugh
R. S. Weiss

October 1, 1993

NASA

National Aeronautics and
Space Administration

Jet Propulsion Laboratory
California Institute of Technology
Pasadena, California

The research described in this publication was carried out by the Jet Propulsion Laboratory, California Institute of Technology, under a contract with the National Aeronautics and Space Administration.

Reference herein to any specific commercial product, process, or service by trade name, trademark, manufacturer, or otherwise, does not constitute or imply its endorsement by the United States Government or the Jet Propulsion Laboratory, California Institute of Technology.

ABSTRACT

The 1993 solar cell calibration balloon flight was completed on July 29, 1993. All objectives of the flight program were met. Forty modules were carried to an altitude of 120,000 ft (36.6 km). Data telemetered from the modules was corrected to 28°C and to 1 AU. The calibrated cells have been returned to 8 participants and can now be used as reference standards in simulator testing of cells and arrays.

ACKNOWLEDGMENT

The authors wish to express appreciation for the cooperation and support provided by the entire staff of the National Scientific Balloon Facility located in Palestine, Texas. The cooperation and patience extended by all participating organizations are greatly appreciated.

CONTENTS

| | |
|---|----|
| 1. INTRODUCTION AND OVERVIEW | 1 |
| 2. PREFLIGHT PROCEDURES | 1 |
| 2.1 MODULE FABRICATION | 1 |
| 2.2 CELL MEASUREMENTS | 2 |
| 2.3 TEMPERATURE COEFFICIENTS AND LEAST SQUARES FITS | 2 |
| 2.4 PANEL ASSEMBLY AND CHECKOUT | 2 |
| 2.5 PRELAUNCH PROCEDURES AT PALESTINE | 2 |
| 3. BALLOON SYSTEM | 6 |
| 3.1 BALLOON DESCRIPTION | 6 |
| 3.2 TOP PAYLOAD | 6 |
| 3.3 BOTTOM PAYLOAD | 7 |
| 4. FLIGHT SEQUENCE | 9 |
| 4.1 PRELAUNCH PREPARATIONS | 9 |
| 4.2 FLIGHT | 11 |
| 4.3 FLIGHT TERMINATION | 11 |
| 5. DATA ANALYSIS | 13 |
| 5.1 COMPUTER ANALYSIS | 13 |
| 5.2 CALIBRATION RESULTS | 15 |
| 5.3 DATA REPEATABILITY | 15 |
| 6. CONCLUSIONS | 15 |
| 7. REFERENCES | 15 |

Figures

| | |
|---|----|
| 1. Photograph of the 1993 Balloon Flight Solar Panel | 3 |
| 2. 1993 Module Location Chart | 4 |
| 3. Tracker Mounted on Aluminum Hoop Assembly With 1993 Complement of Flight Modules | 5 |
| 4. Block Diagram of Balloon Telemetry System | 8 |
| 5. Flight Train Configuration | 10 |
| 6. Balloon Launch | 12 |
| 7. 1993 Balloon Flight Profile | 14 |

Tables

| | |
|---|----|
| 1. 1993 Balloon Flight 7/29/93 120,000 ft, RV = 1.0152078, Flight No. 1530P | 16 |
| 2. Repeatability of Nine Standard Solar Cell Modules Over a 20-year Period | 17 |

"Good judgement comes from experience, and experience comes from bad judgement."
Barry LePatner

1. INTRODUCTION AND OVERVIEW

The primary source of electrical power for unmanned space vehicles is the direct conversion of solar energy through the use of solar cells. As advancing cell technology continues to modify the spectral response of solar cells to utilize more of the Sun's spectrum, designers of solar cells and arrays must have the capability of measuring these cells in a light beam that is a close match to the solar spectrum. The solar spectrum has been matched very closely by laboratory solar simulators. But the design of solar cells and the sizing of solar arrays require such highly accurate measurements that the intensity of these simulators must be set very accurately. A small error in setting the simulator intensity can conceivably cause a disastrous missizing of a solar panel, causing either a premature shortfall in power or the launch of an oversized, overweight solar panel.

The Jet Propulsion Laboratory (JPL) solar cell calibration program was conceived to produce reference standards for the purpose of accurately setting solar simulator intensities. The concept was to fly solar cells on a high-altitude balloon, to measure their output at altitudes near 120,000 ft, to recover the cells, and to use them as reference standards. The procedure is simple. The reference cell is placed in the simulator beam, and the beam intensity is adjusted until the reference cell reads the same as it read on the balloon. As long as the reference cell has the same spectral response as the cells or panels to be measured, this is a very accurate method of setting the intensity. But as solar cell technology changes, the spectral response of the solar cells changes also, and reference standards using the new technology must be built and calibrated.

Until the summer of 1985, there had always been a question as to how much the atmosphere above the balloon modified the solar spectrum. If the modification was significant, the reference cells might not have the required accuracy. Solar cells made in recent years have increasingly higher blue responses, and if the atmosphere has any effect at all, it would be expected to modify the calibration of these newer blue cells much more so than for cells made in the past.

In late 1984, a collection of solar cells representing a wide cross section of solar cell technology was flown on the shuttle Discovery as a part of the Solar Cell Calibration Facility (SCCF) experiment. The cells were calibrated as

reference cells on this flight by using procedures similar to those used on the balloon flights. The same cells were then flown on the 1985 balloon flight and remeasured. Since the two sets of measurements gave nearly identical results (see reference 1), the reference standards from balloon flights may continue to be used with high confidence.

JPL has been flying calibration standards on high-altitude balloons since 1963 and continues to organize a calibration balloon flight at least once a year. The 1993 flight was the 46th flight in this series. The 1993 flight incorporated 40 solar cell modules from eight different participants. The payload included Si, amorphous Si, GaAs, and CdTe cells. The flight included 11 cells that were fitted with narrow bandpass filters at 11 different wavelengths. The latter cells are intended to become standards for use in the calibration of spectral response measurement equipment.

2. PREFLIGHT PROCEDURES

2.1 MODULE FABRICATION

The cells were mounted by the participants or by JPL on JPL-supplied standard modules according to standard procedures developed for the construction of reference cells. The JPL standard module is a machined copper block on which a fiberglass circuit board is mounted. The circuit board has insulated solder posts which are used for making electrical connections to the solar cell and to a load resistor. This circuit board can be modified to include two binding posts and a jumper in series with one of the leads to the resistor. After flight calibration, the jumper can be removed and replaced with current pickoff probes for use on pulsed xenon simulators that may require a current input. The assembly is painted with either high-reflectance white or low-reflectance black paint. The resistor performs two tasks. First, it loads the cells near short-circuit current, which is the cell parameter that varies in direct proportion to light intensity. Second, it scales the cell outputs to read near 100 mV during the flight, which matches a constraint imposed by the telemetry electronics. Load resistance values are 0.5 ohm for a 2 x 2 cm cell, 0.25 ohm for a 2 x 4 cm cell, etc. The load resistors are precision resistors (0.1%, 20 ppm/°C) and have a resistance stability equal to or better than $\pm 0.002\%$ over a 3-year period. The solar cells are permanently glued to the body of the machined copper block with RTV 560 or its equivalent. This gives a good thermal conductivity path between cell and copper

block, while providing electrical insulation between the rear surface of the solar cells and the block.

2.2 CELL MEASUREMENTS

After the cells were mounted on the copper blocks, the electrical output of each cell module was measured under illumination by the JPL X25 Mark II solar simulator. For these measurements, the simulator intensity was set by using only one reference cell--no attempt was made to match the spectral response of the reference standard to the individual cell modules. The absolute accuracy of these measurements is therefore unknown, but the measurements do allow checking of the modules for any unacceptable assembly losses or instabilities. After the balloon flight, the cells were measured in exactly the same way to check for any cell damage or instabilities that may have occurred as a result of the flight.

2.3 TEMPERATURE COEFFICIENTS AND LEAST SQUARES FITS

The temperature coefficients of the mounted cells were also measured before the flight. The modules were mounted in their flight configuration on a temperature-controlled block in a vacuum chamber. Outputs were measured at 25, 35, 45, 55, 65, and 75°C under illumination with the X25 simulator. The temperature coefficients of the cell modules were computed by fitting the output vs temperature relationship with a linear least squares fit.

2.4 PANEL ASSEMBLY AND CHECKOUT

After the electrical measurements were completed, the modules were mounted on the solar panel and connected electrically. Figure 1 is a photograph of the modules after completion of these steps, and Figure 2 is a diagram that identifies the modules in the photograph by their serial numbers. After completion of the panel assembly, the panel and tracker together were given complete functional tests in terrestrial sunlight. The assembled tracker and panel were placed in sunlight on a clear, bright day, and checked for the tracker's ability to acquire and track the Sun while each cell module was checked for electrical output. After these tests were completed satisfactorily, the assembly was shipped to the National Scientific Balloon Facility (NSBF) in Palestine, Texas, for flight.

2.5 PRELAUNCH PROCEDURES AT PALESTINE

The NSBF was established in 1963 at Palestine, Texas. This location was chosen because it has favorable weather conditions for balloon launching and a large number of clear days with light surface winds. The high-altitude winds in

this part of the country take the balloons over sparsely populated areas so the descending payloads are unlikely to cause damage to persons or property. The JPL calibration flights have flown from the Palestine facility since 1973. The flights are scheduled to fly in the June to September time period, since the Sun is high in the sky at that time of year, and the sunlight passes through a minimum depth of atmosphere before reaching the solar modules.

Upon arrival at Palestine, the tracker and module payload were again checked for proper operation. This included a checkout in an environmental test chamber wherein the tracker, data encoder, and voltage reference box were all tested as a system. The chamber was pumped down to a pressure of ≈ 40 mb [corresponding to an altitude of 65,000 ft (19.8 km)], cooled to -50°C. The system was tested at 10° increments during the cool down. Then, the assembly was removed from the environmental chamber and a room-temperature, end-to-end check was performed on the payload, telemetry, receiving, and decoding systems. The four output voltage levels of the voltage reference box were wired into the telemetry stream along with the module outputs. The analog-to-digital converter system was calibrated by recording these four voltage levels as they were input to the system and as they were converted, decoded, and sent through the system as digital output values. The thermistor channels were calibrated by replacing each thermistor, in turn, with a known calibration resistor while the entire system was operating. Eleven resistors are used in this procedure to produce calibrations at 10 deg increments over the 0 to 100°C range. The checkout was completed by monitoring the system over a period of 2 to 3 hours to make sure that no stability problems occurred.

After all the checkouts and calibrations were performed, the tracker was mounted onto the aluminum tubular hoop assembly which will ride on the top portion (or apex) of the balloon. Figure 3 is a photograph of the tracker mounted on the hoop assembly. The solar panel is shown with a typical complement of calibration modules.

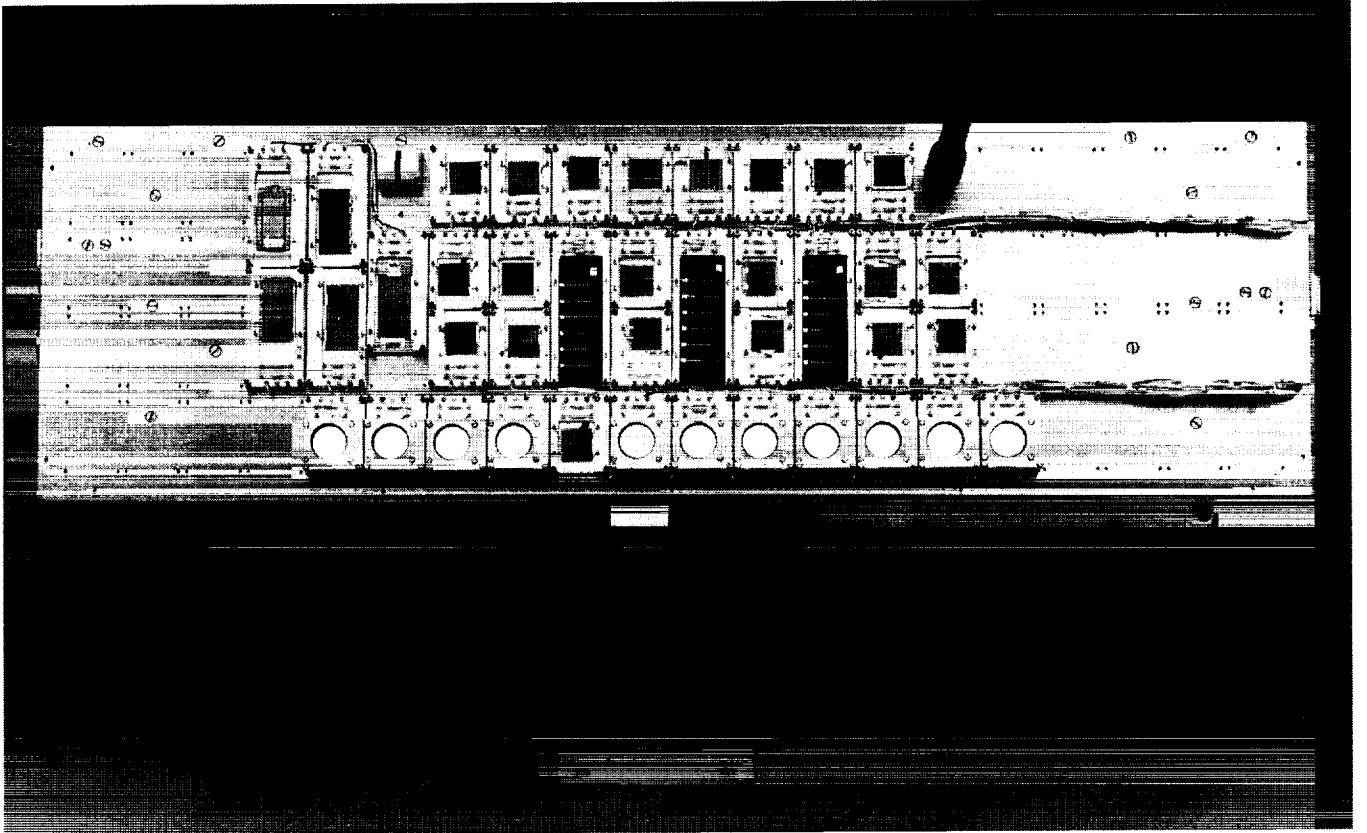
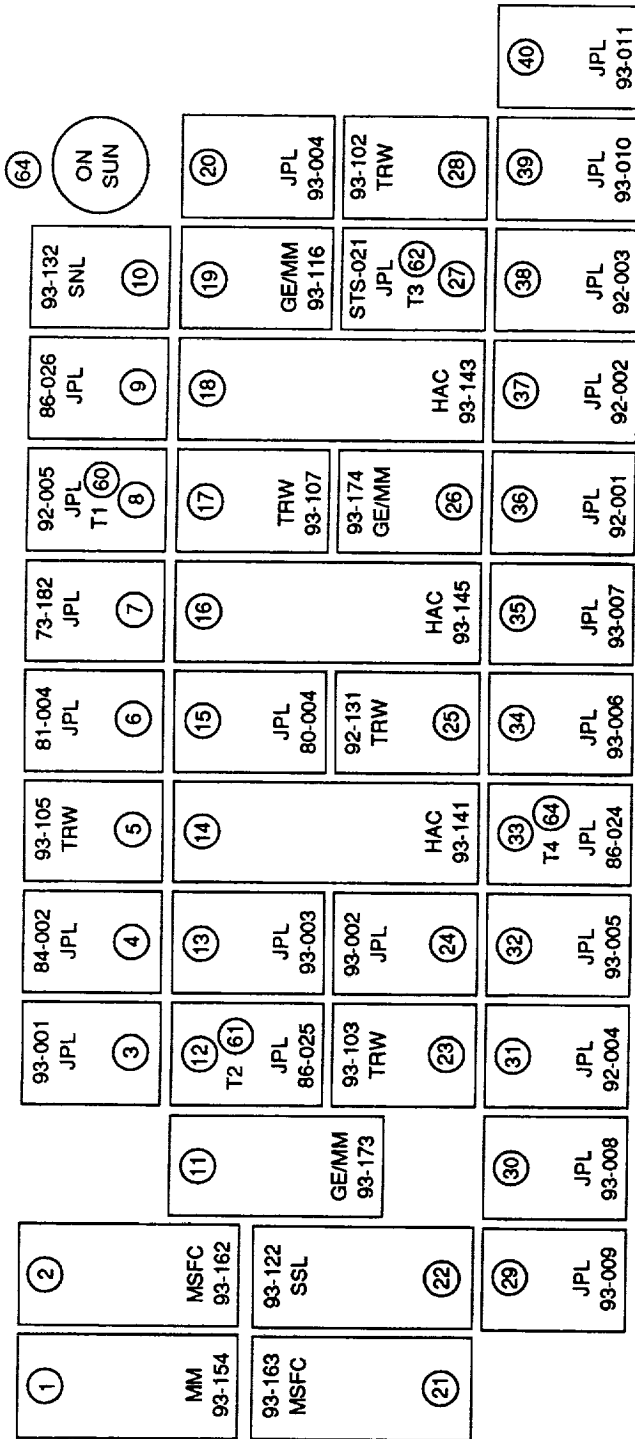


Figure 1. Photograph of the 1993 Balloon Flight Solar Panel



- ⑥0 THERMISTOR 1
- ⑥1 THERMISTOR 2
- ⑥2 THERMISTOR 3
- ⑥3 THERMISTOR 4

Figure 2. 1993 Module Location Chart

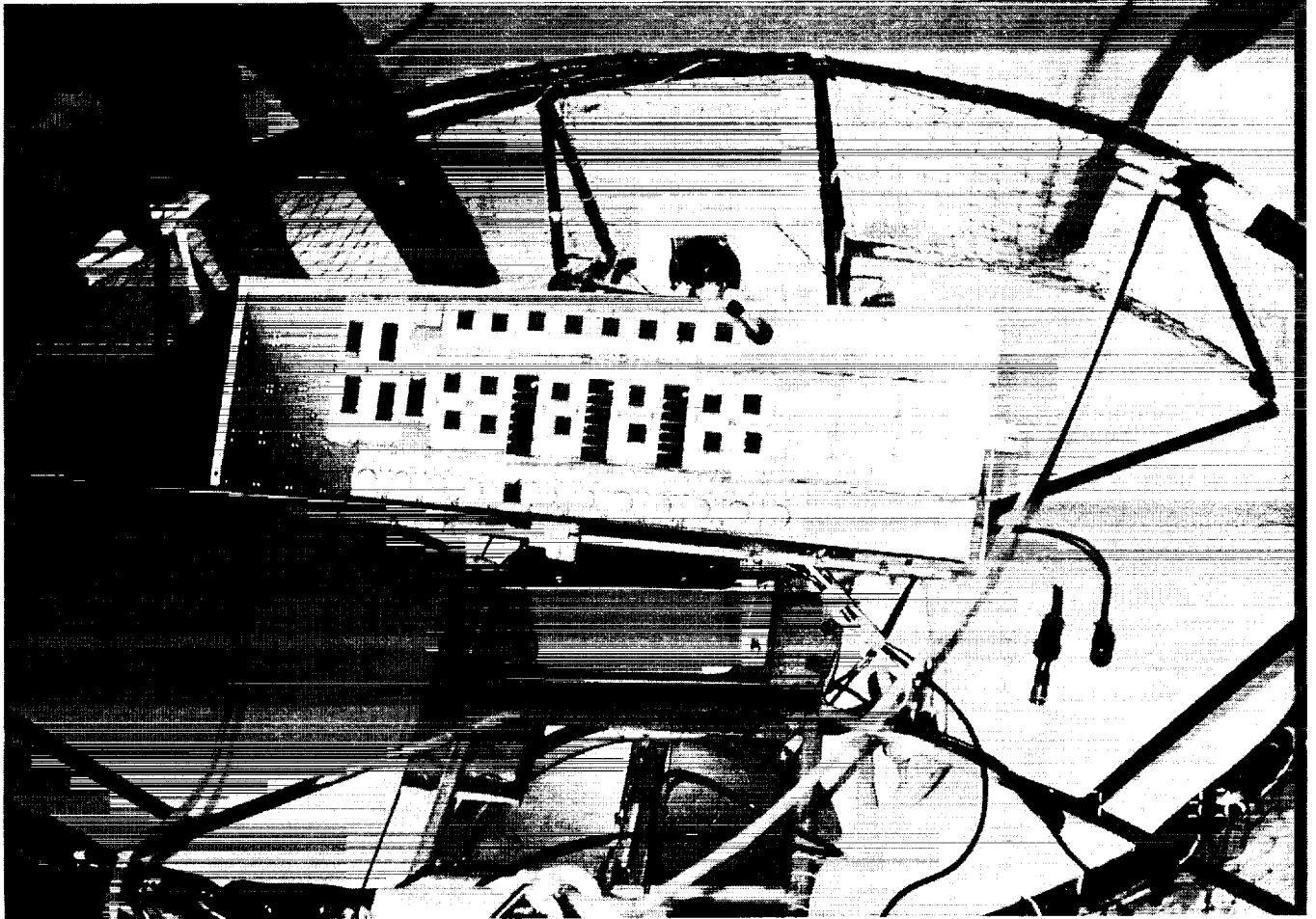


Figure 3. Tracker Mounted on Aluminum Hoop Assembly With 1993 Complement of Flight Modules

3. BALLOON SYSTEM

The main components of the balloon flight system were (1) the apex-mounted hoop assembly that contains the experimental package, the data encoder, the recovery system, and the camera package; (2) the balloon; and (3) the lower payload that contains the telemetry and power systems.

3.1 BALLOON DESCRIPTION

The balloon used for the JPL solar cell calibration high-altitude flights had a volume of 3.46 million ft³ (98,000 m³). The balloon manufacturers use 0.8 mil (20 μ m) polyethylene films designed specifically for balloon use, either Stratofilm 372 (Winzen) or Astrofilm E2 (Raven). The balloon alone weighed 695 lb (316 kg). The balloon was designed to lift itself and a payload weight of up to 725 lb (330 kg), distributed between the bottom and top payloads, to a float altitude of 120,000 ft (36 km). At float altitude, the balloon will have a diameter of roughly 188 ft (59 m). To electrically connect the top and bottom payloads, a multiconductor cable was built into the balloon during its manufacture. The balloon was built with an internal rip line designed to rip a hole in the side of the balloon for termination of the flight. A special structure was built into the top of the balloon for attaching the top payload. Two poppet valves incorporated into this mounting structure are commanded to open and release helium from the balloon at the end of the flight. The poppet valves act as a backup to the rip line.

Trying to inflate and launch a balloon with a sizable weight attached to its top is similar to an inebriated moose trying to tiptoe down a barbed wire fence. A tow balloon tied to the top payload was used during the inflation and launch phases to add stability and to keep it on top. This smaller balloon, about 31,000 ft³ (880 m³), is designed to lift about 160 lb (73 kg). The tow balloon was cut loose from the top payload after the launch as soon as the main balloon stabilized and the launch-induced oscillations damped out.

3.2 TOP PAYLOAD

The top payload consists of the tracker, solar panel, voltage reference box, multiplexer, data encoder, single-frame movie camera, clock, descent parachute, battery power supply for the tracker and data encoder, relay box, and tracking beacon. All these items were mounted to the aluminum hoop assembly shown in Figure 3. The hoop assembly, with appropriately placed Styrofoam crush pads, served the following functions:

- (1) Permitted the top-mounted payload to "float" on top of the balloon and minimized billowing of balloon material around the top payload.
- (2) Served as the mounting surface for the balloon's top-end fitting.
- (3) Provided a convenient point for attaching the tow balloon and the descent parachute.
- (4) Acted as a shock damper to protect and minimize damage to the top payload at touchdown.

The complete apex-mounted hoop assembly, as flown, weighed approximately 110 lb (50 kg) and descended as a unit by parachute at flight termination.

The sun tracker, shown in Figure 3, is capable of orienting the solar panel toward the Sun, compensating for the motion of the balloon by using two-axis tracking in both azimuth and elevation. The tracker has the capability to maintain its lock onto the Sun to within ± 1 deg. To verify that the tracker was operating properly, the output of an on-sun indicator was constantly monitored during flight by feeding its output to the multiplexer and entering its signal into the telemetry stream. The on-sun indicator consists of a small, circular solar cell mounted at the bottom of a collimator tube, 7 in. (17.8 cm) long, with an aperture measuring 0.315 in. (0.8 cm) in diameter. The indicator was attached to the solar panel so that it pointed at the Sun when the panel was perpendicular to the Sun. The output of the on-sun indicator falls off very rapidly as the collimator tube points away from the Sun and provides a very sensitive indication of proper tracker operation.

A reflection shield was attached to the panel to prevent any stray reflected light from reaching any of the modules. This shield was made of sheet aluminum and attached to three edges of the solar panel. The shield is the U-shaped, black object shown on the panel in Figure 3.

The solar cell modules were mounted onto the sun tracker platform with an interface of Apiezon H vacuum grease and held in place with four screws. The grease was used to achieve a highly conductive thermal contact between the modules and the panel and to smooth out the temperature distribution over the solar panel as much as possible.

The solar panel temperature was monitored using thermistors. Some of the solar cell modules were constructed with calibrated precision thermistors embedded in the copper substrate directly beneath the solar cell. Four

of these modules were mounted on the solar panel at strategic locations so their temperature readings gave an accurate representation of panel temperature. Placement of these modules on the panel is shown in Figure 2.

The pulse code modulation (PCM) data encoder amplified the analog signals from the solar cells, thermistors, on-sun indicator, and reference voltages, then performed an analog-to-digital conversion. The encoder had a programmable control unit that was used to set bit rate, bits per word, parity, analog-to-digital conversion, and format. Two 32-channel multiplexers allow sampling of up to 64 data channels and amplify the low-level signals from the experimental package. The amplifier was designed to process voltage signals at input levels up to 100 mV. The multiplexer stepped through the various channels at a rate of two scans per second, i.e., every data channel is read twice each second.

An ultrawide-angle, single-frame movie camera mounted at the perimeter of the aluminum hoop provided visual documentation of tracker operation. A battery-powered timer activated the shutter at 10-second intervals, so that 50 ft of 8 mm movie film is sufficient to record the entire flight from launch to landing. A windup clock was placed in the camera's field of view for correlation of tracker operation with the telemetered data. The pictures provide a complete record of ascent, tracker operation at float altitude, descent, touchdown, and post-touchdown events.

A tracking or locator beacon was attached to the hoop assembly. This beacon, similar to those used for tracking wild animals in their natural habitat, consists of a low-wattage transmitter which sends short 160 MHz pulses at the rate of about one per second. A hand-held directional antenna and a battery-powered receiver are used inside the chase plane and on the ground for locating the transmitter. This beacon has been very useful in locating this very small payload in a very large open range.

3.3 BOTTOM PAYLOAD

The bottom payload was entirely furnished by the NSBF. It consists of a battery power supply, a ballast module for balloon control, and an electronics module known as the consolidated instrument package (CIP).

Power for operating most of the electrical and electronic equipment on the balloon was supplied by a high-capacity complement of lithium batteries. This supply, furnishing 28 Vdc regulated power and 36 Vdc unregulated power, powered all the instruments in the CIP. Several other small

battery sources were used at various locations on the balloon for instruments that require small amounts of power. For example, the tracker and data encoder, the tracking beacons, the voltage reference box, and the camera timer all had individual battery power supplies. All batteries were sized to supply power for at least twice the expected duration of a normal flight.

High-altitude balloons tend to lose helium slowly during the course of the flight. As a consequence, a helium balloon will tend to reach float altitude and then begin a slow descent. To counteract this tendency, a ballast system was included as part of the bottom payload. It contained approximately 100 lb (45 kg) of ballast in the form of very fine steel shot. The shot may be released in any desired amount by radio command. By proper use of this system, float altitude may be maintained to within $\pm 2,000$ ft (± 600 m).

The telemetry system was contained in the CIP. A block diagram of the telemetry system is shown in Figure 4. The system sent all data transmissions concerning the flight over a common RF carrier. The CIP also contained a command system for sending commands to the balloon for controlling scientific payloads or for controlling the housekeeping functions on the balloon. Specifically, the CIP contained the following equipment:

- (1) MKS pressure transducers
- (2) Subcarrier oscillators, as required
- (3) L-band FM transmitter
- (4) High-frequency tracking beacon transmitter
- (5) Transponder for air traffic control tracking
- (6) PCM command receiver-decoder
- (7) Loran receiver
- (8) GPS receiver

The altitude of the balloon was measured with a capacitance-type electronic transducer, which read pressure within the range of 1,020 to 0.4 mbar (102,000 to 40 N/m²) with an accuracy of 0.05%. The transducer produced a dc level that was encoded as PCM data and decoded at the receiving station into pressure, and then the altitude was calculated from the pressure reading.

The Loran, and Global Positioning Satellite (GPS) navigation systems were used for flight tracking. An on-board receiver was used to receive these signals for retransmission to the processor in the ground station. This system can provide position data to an uncertainty of less than 1 mi (1.6 km). The Loran and GPS signals were multiplexed into the telemetry stream and updated every 8 seconds.

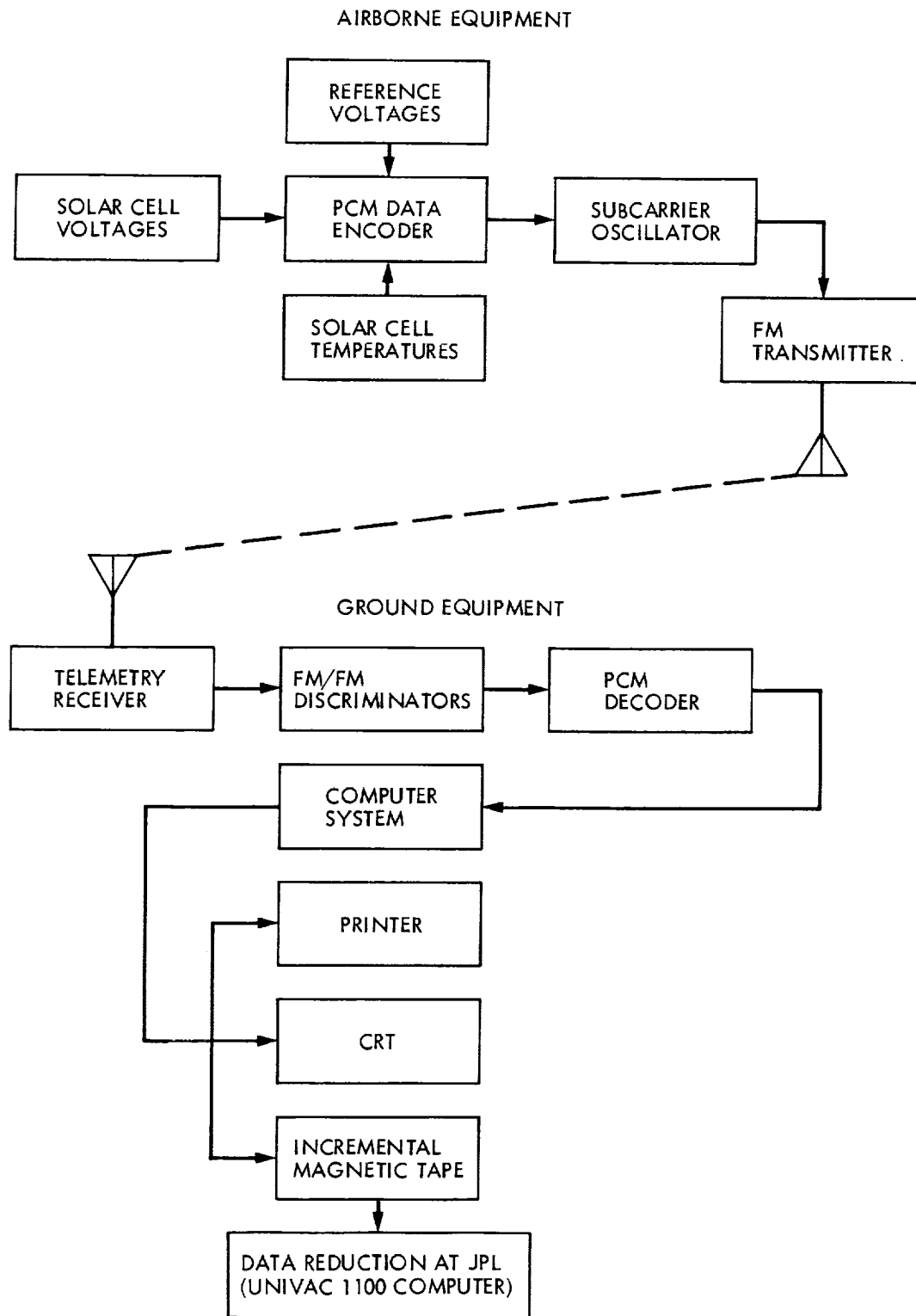


Figure 4. Block Diagram of Balloon Telemetry System

As previously mentioned, all the telemetry data was sent to the ground in the form of pulse code modulation. A UHF L-band transmitter in the CIP was used to generate the RF carrier. The L-band carrier was modulated by the pulse code and sent to the receiving station at Palestine.

An aircraft-type transponder was flown so that Air Traffic Control (ATC) could read the balloon's location on their radar systems during the descent portion of the flight. ATC was helpful in relaying to the recovery aircraft the exact position of the bottom payload during its descent on the parachute.

The purpose of the PCM command system is to send commands to the balloon, e.g., to turn the tracker on or off, terminate the flight, release ballast, etc. It was designed to reject false commands and was highly reliable in operation. The data was encoded on a frequency-shift-keyed audio carrier. This signal was then decoded into data and timing control. Each command consisted of a double transmission of the data word. Both words must be decoded and pass a bit-by-bit comparison before a command can be executed. Commands may be sent to the balloon from either the ground station at Palestine or from the recovery airplane.

The lower payload is suspended from the balloon by an 8.5 m diameter parachute. The top end of the parachute was fastened to the bottom of the balloon, and the lower payload (which contained the CIP, the battery power supply, and the ballast) was attached to the shroud lines. Appropriate electrical cables and breakaway connectors were rigged in parallel with the mechanical connections. The whole bottom assembly was designed to break away from the balloon and fall to Earth while suspended from the parachute at termination of the flight.

4. FLIGHT SEQUENCE

4.1 PRELAUNCH PREPARATIONS

The balloon launchpad at the NSBF is a large circular area, 2,000 ft (600 m) in diameter. In the center of this large circle is another circular area, solidly paved, measuring 1,000 ft (300 m) in diameter. Grass is planted in the area between the two circles, and a paved road surrounds the larger circle. Paved radials extend from the perimeter road toward the launchpad.

When all prelaunch preparations had been completed and the staff meteorologist had predicted favorable weather and winds at Palestine and for some 300 mi (480 km) downrange, the equipment was taken to the launch site. (Launches from Palestine are only authorized when the

predicted termination point is at least 200 mi West of Palestine).

At the launch pad, the main balloon, protected by a plastic sheath, was laid out full-length on the circular paved area. It was aligned with the direction of the wind and positioned so that the top of the balloon is on the upwind side. The top end of the balloon was passed under, behind, and over the top of a large, smooth, horizontal spool mounted on the front end of the spool vehicle. One end of this launching spool was hinged to the spool vehicle. The other end of the spool had a latch that could be released by a trigger mechanism. After the balloon was passed over the spool, the spool was pushed back to engage the latch so that the spool trapped the balloon. The top 10 m or so of the balloon was pulled forward from the spool, allowing the top payload to rest on the ground. It is this top 10 m of balloon that later receives the helium gas during inflation. The helium will form a kind of bubble in the part of the balloon above the launching spool. After the launching spool was latched, final preparations of the top payload began. The tow balloon was attached to the hoop with nylon lines, the clock was wound, the camera was energized, and a final checkout of the tracker and data encoder was performed.

The launch sequence began by inflating the tow balloon with helium. The main balloon was then inflated by passing a predetermined volume of helium through two long fill-tubes and into the balloon. Figure 5 shows the configuration of the flight train at this stage of preparation. The balloon was launched by triggering the latch on the launching spool. When the latch was released, a stout spring caused the free end of the spool to fly forward, rotating about the hinge, which released the balloon. As the balloon rose, the launch vehicle at the lower end of the balloon began to move forward (downwind). After the driver of the launch vehicle had positioned the vehicle directly below the balloon and had his vehicle going along at the same speed as the balloon, he released the latch on the pin and the lower payload was released. Figure 6 shows the balloon system and the launch vehicle a few seconds after release of the launching spool just as the downwind launch vehicle began to move. As soon as the main balloon quit oscillating, a signal was sent from the launchpad, which triggered an explosive charge. This released the tow balloon, and the launch sequence was complete.

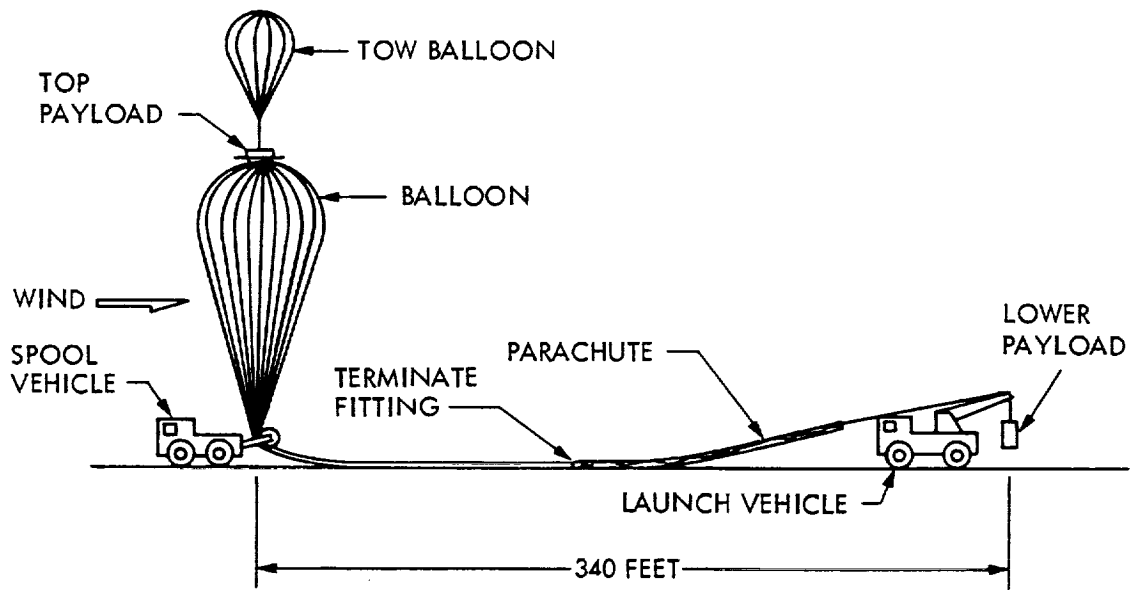
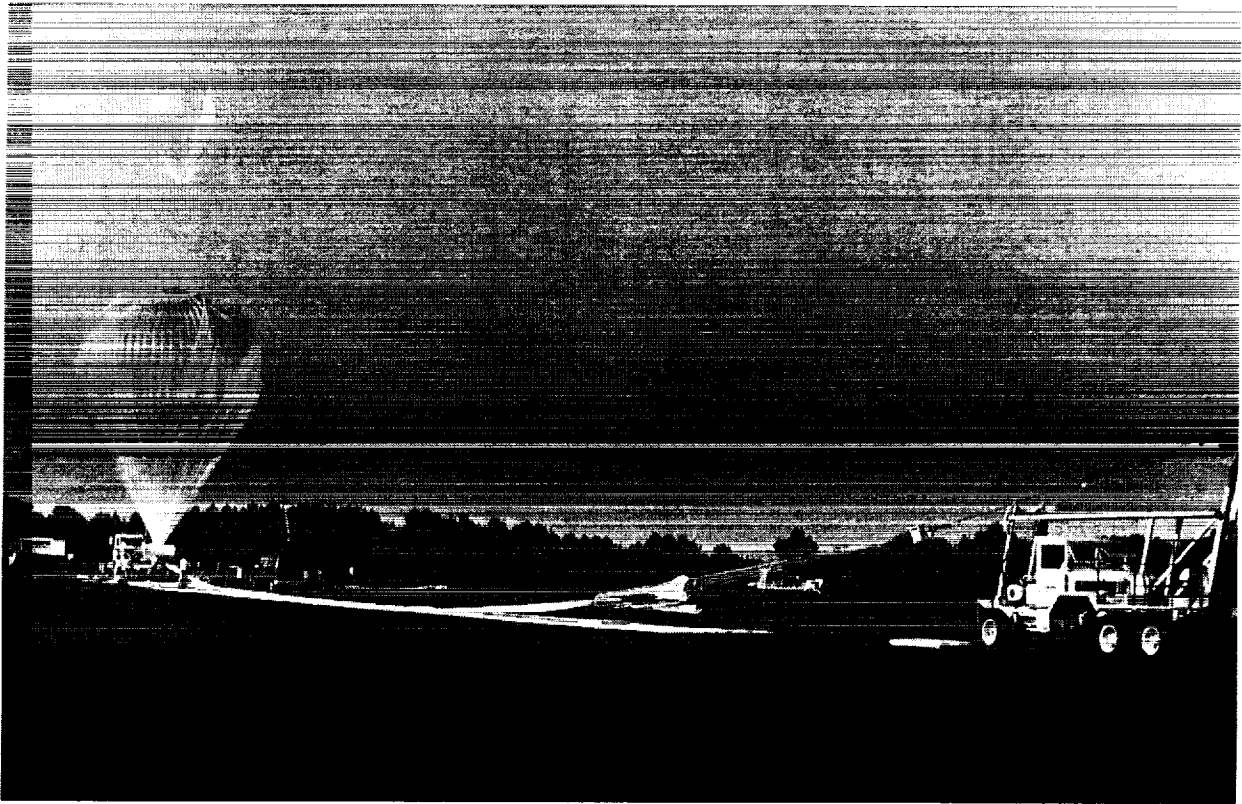


Figure 5. Flight Train Configuration

4.2 FLIGHT

The balloon ascended at a rate of approximately 900 ft/min (4.6 m/s) and reached float altitude after approximately 2 hours. During the ascent, the flight controller at Palestine maintained a constant contact with ATC. Data from the onboard navigational system was continuously given to ATC so that air traffic in the area could be vectored around the balloon.

After the balloon had been launched, solar cell voltages interspersed with reference calibration voltages and thermistor voltages were fed into the telemetry system. These voltages were converted to PCM and were transmitted to the NSBF ground station along with the navigational, altitude, and other information from the CIP. At the ground station, the signals were decoded, recorded, and displayed in real time for monitoring of the flight. The balloon reached float altitude at 1424 GMT, which was approximately 4 hours before solar noon. The tracker was turned on by telemetry command about 1 hour after reaching float altitude. Tracker operation was monitored by observing the output of the on-sun indicator and the outputs of about half the solar cell modules. Data was recorded from time of launch at 1204 GMT through 1850 GMT, when the flight was terminated. Solar noon occurred at approximately 1830 GMT for this flight.

4.3 FLIGHT TERMINATION

Shortly after launch, a ground recovery crew began driving toward the expected termination area in a special recovery truck. Approximately 2 hours after the balloon reached float altitude, the recovery airplane took off from Palestine with an experimenter and an observer aboard. This airplane was equipped with a radio system that allowed the crew to maintain constant communication with the balloon base and with the ground recovery crew. The airplane also had a full command system so that it could send commands to the balloon.

During the summer months, the winds at altitudes above 80,000 ft (24 km) blow from east to west at speeds of about 50 knots (25 m/s), so the airplane had to fly about 200 mi (330 km) west of Palestine to be in position for recovery. The pilot could fly directly toward the balloon at any time by flying toward the telemetered location of the balloon. This position information was generated by the Loran and GPS systems on the balloon, telemetered to the Balloon Base at Palestine, and relayed from there to the airplane. The observer in the recovery airplane shared the responsibility for termination of the flight with the launch director in the NSBF control tower at Palestine. Before leaving Palestine, the recovery personnel had received a set

of descent vectors from the meteorologists. The descent vectors are estimates of the trajectories that the payloads should follow as they descend by parachute. Upon receiving word from Palestine that the experimenter had sufficient data, the pilot flew under the balloon to double check the accuracy of the GPS data. Using the descent vectors, he then plotted where the payloads should come down. He also established contact with ATC. When ATC advised that the descending payloads would not endanger air traffic, and when the descent vector plots showed that the payloads would not come down in an inhabited area, the observer aboard the airplane sent the commands to the balloon which terminated the flight.

The termination sequence consisted of first sending a command that disconnected power from the tracker and data encoder. Next a command was sent that cut the electrical cable running from the bottom payload to the top payload. This command simultaneously cut the cables holding the top payload onto the top of the balloon and opened the poppet valves on the top of the balloon. A second command released the bottom parachute from the balloon, which allowed the bottom payload to fall away and caused the balloon to become top-heavy. As the bottom payload fell, a ripcord attached to the top of the parachute opened a large section in the balloon. The balloon collapsed, the top payload fell off the balloon, its parachute opened, and all three objects began their descent.

The top payload descended on its chute for 38 minutes (average descent rate = 3158 ft/min), and the bottom payload descended on its chute for 63 minutes (average descent rate = 1904 ft/min). During this time, the pilot monitored the position of both the top and bottom payloads by visual reference. After reaching the ground, all three items had to be found. Since the payloads were observed at impact, locating them was not a problem, but a brief search pattern had to be flown in order to locate the balloon. The precise locations of all three items were established by recording their coordinates on a hand-held GPS unit. Once the impact locations were established from the air, the ground recovery crew was furnished with the GPS data and rough sketches of each location.

Figure 7 is the flight profile for the 1993 balloon flight (No. 1530P in the nomenclature of the NSBF). The plot shows altitude vs time from the time of launch until touchdown. The points are plotted at approximately 10-minute time intervals. The touchdown site was south of San Angelo, Texas near the town of Eldorado, approximately 305 mi (491 km) from the launch site. The total flight duration from launch until the terminate command was sent was ≈ 7 hours. The period of time

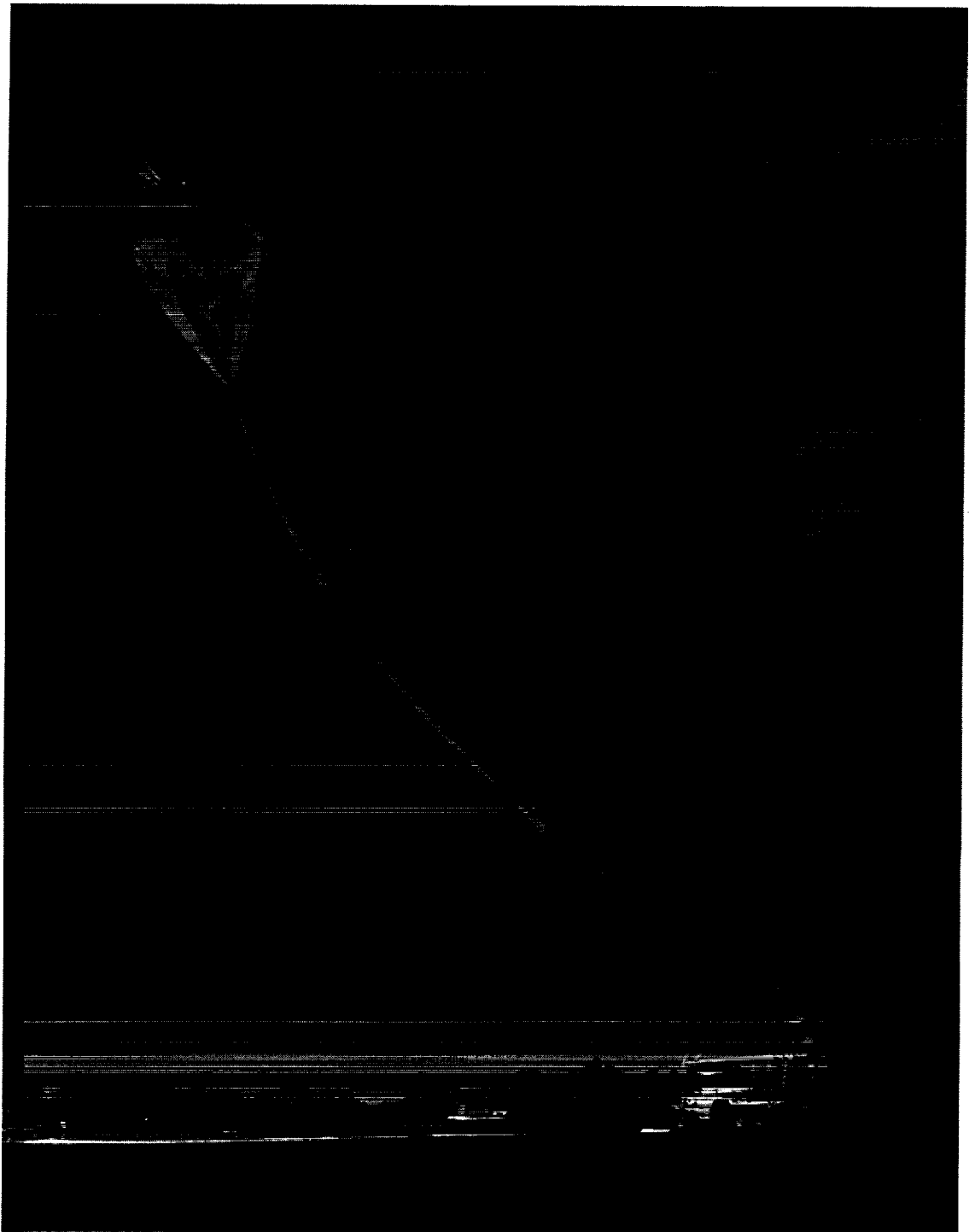


Figure 6. Balloon Launch

during which computer analysis of the flight data occurred is also shown on the Figure.

5. DATA ANALYSIS

The computer analysis was performed at JPL by using the Unisys 1100 computer. The program read the raw data from the magnetic tape produced during the flight, then corrected the cell data for temperature and Sun-Earth distance according to the formula:

$$V_{28,1} = V_{T,R}(R^2) - A(T - 28)$$

where

- $V_{T,R}$ = measured module output voltage at temperature T and distance R.
- R = Sun-Earth distance in astronomical units (AU).
- A = module output temperature coefficient.
- T = module temperature in degrees C.

The remainder of this section describes the details of performing the above corrections and computing calibration values for the cells.

5.1 COMPUTER ANALYSIS

The computer program read data from the magnetic tape one record at a time. Each record contained 16 scans of data plus a ground frame. Each scan of data consisted of two synch words followed by a reading of each of the 64 data channels. The ground frame contained the date and time of the scan followed by the latitude, longitude, and pressure, as measured by instruments on the balloon. The program first checked the ground frame to see whether the record fell within the allowed data analysis time. (The allowed data analysis time window is an input to the program set by the parameters MINTIM and MAXTIM.) The computer rejected the entire frame if the time of the current record fell outside the time window or if it could not read the time properly. The computer read records within the time window until it had accumulated 200 scans. Each set of 200 scans is called a pass. At this point, the data was in PCM counts. The PCM data for each channel was averaged, then a screening procedure was used to reject scans containing questionable data. For example, scans were rejected if the on-sun indicator was lower than a threshold value (input parameter OSMIN). Scans were also rejected if the PCM count for a data channel was not within the allowable PCM count range, if there was too large a count deviation on any channel from one scan to the next, or if there was an unrecoverable problem in reading the tape.

The PCM data was next converted to engineering units. The program has a provision for doing this in any one of four different ways. The simplest and most commonly used method will be described here. During the calibration of the telemetry system, the output of the telemetry system vs the input from the voltage reference box was recorded to produce a table of mV input vs PCM count output. Similarly, for the thermistor channels, a series of resistors was connected one by one across a thermistor channel, and the resulting PCM count for that channel was recorded. Since the temperature corresponding to each resistance value was known, the construction of a PCM count vs temperature table was possible. This procedure was repeated for all thermistor channels, and a calibration table was constructed for each thermistor channel. Both calibration tables were supplied to the computer program. During conversion of solar cell data to mV, the computer performed a linear interpolation in the PCM vs mV table. At the completion of the initial computer analysis run, the output values of each channel corresponding to voltage reference levels were checked. If they held constant during the flight (they normally read constant to within ± 1 PCM count out of 1,000), the use of the simple linear interpolation scheme was continued for the final data analysis. Since the relationship between thermistor resistance and temperature is nonlinear, a third-degree polynomial was used for the interpolation of the temperature values.

At the end of each pass, four averages were computed for each channel: (1) an initial average based on all acceptable scans, (2) a corrected average using all data falling within a specified fractional deviation (input parameter ADEV) of the initial averages, (3) the corrected average multiplied by the square of the Earth-Sun radius vector (in AU) for the day of the flight (reference 2), and (4) a final average with all the above corrections plus a temperature correction to 28°C. This final correction used the values of the temperature coefficients measured in the laboratory (input parameters TPCOEF). This process completes the data analysis for one pass of data. The entire procedure was repeated by returning to the tape-reading routine and reading another pass (200 scans) of data. The screening and averaging routines were also performed on this pass. This procedure was iterated until 30 passes of data had been analyzed or until MAXTIM was exceeded. This resulted in 6,000 data points for each cell module on the flight.

In addition to the averages taken after each pass, an overall summary matrix was constructed that contained the fully corrected averages for each channel after each pass. A row of entries was added to this matrix after each pass.

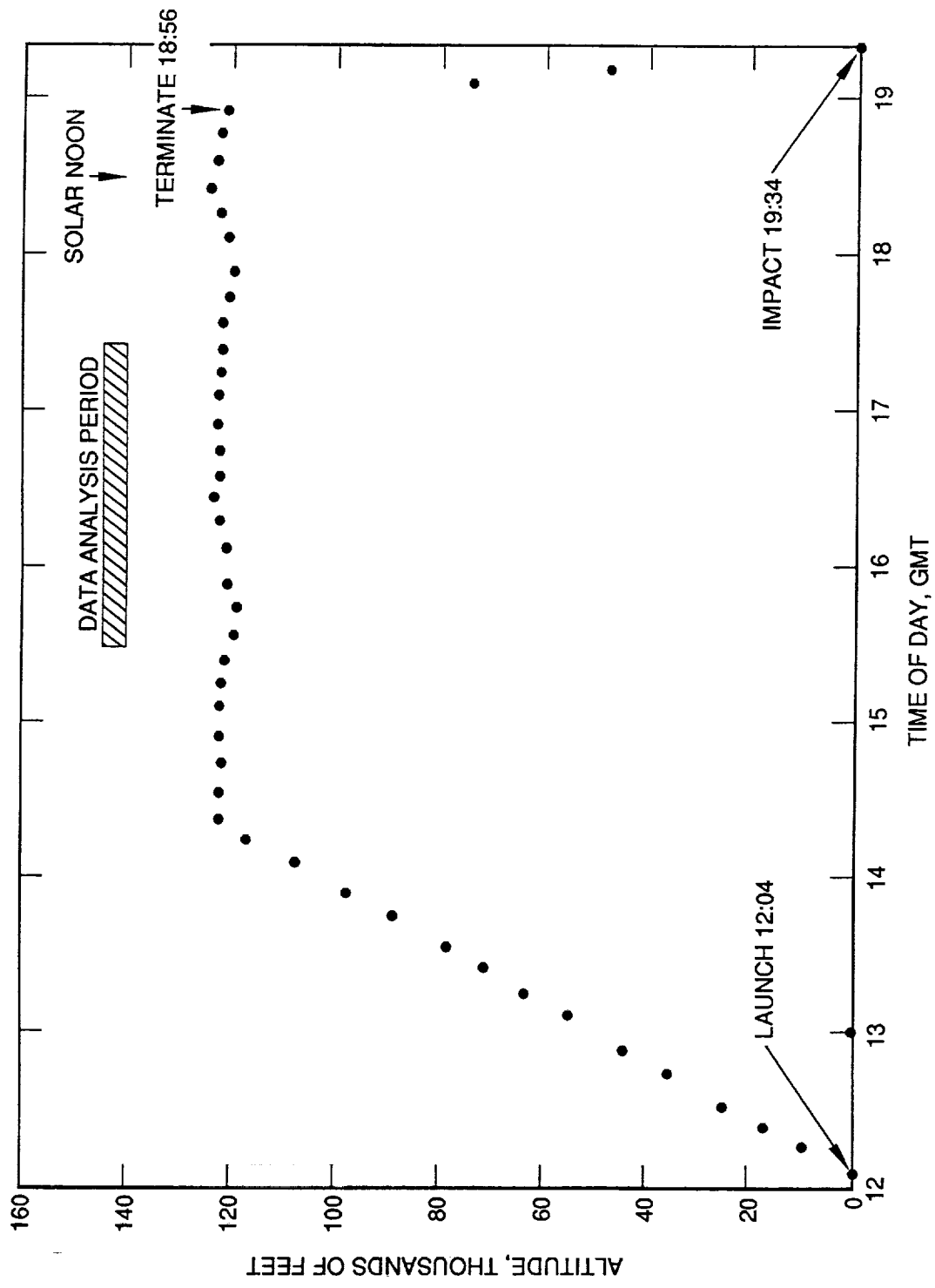


Figure 7. 1993 Balloon Flight Profile

After all passes had been completed, an overall average and standard deviation were computed for each channel. These overall averages of 6,000 readings are the reported calibration values for the modules.

5.2 CALIBRATION RESULTS

Table 1 reports the calibration values of all the cells calibrated on the 1993 balloon flight corrected to 28°C and to 1 AU. The table also reports the standard deviation of the 6,000 measurements, the preflight and postflight readings of each module in the X25 simulator, a comparison of the preflight with the postflight simulator readings, and a comparison of the preflight simulator readings with the balloon calibration readings. The table also reports the temperature coefficients measured for each module in the laboratory.

5.3 DATA REPEATABILITY

Several standard modules have been flown repeatedly over the 31-year period of calibration flights. Module BFS-17A, which had flown on 41 flights, was damaged in 1990 and is no longer available. In its history of 41 flights, the calibration values for BFS-17A averaged to a value of 60.180, with a standard deviation of 0.278 (0.46%). In addition to giving a measure of the consistency of the year-to-year measurements, BFS-17A also provided insight into the quality of the solar irradiance falling on the solar panel, with regard to uniformity, shadowing, or reflections. This cell had been mounted in various locations on the panel over the years. Nevertheless, its readings were always consistent, which verified that there are no uniformity, shadowing, or reflection problems with the geometry of this system.

We have identified a group of solar cells that will be used as replacements for the function served by BFS-17A. Some cells from this group will be flown every year so that we can continue our year-to-year continuity checks. We chose nine samples from this group for flight in 1993. Six of these cells were Si cells, one of which was flown on the shuttle. Two cells were GaAs cells and one was a GaAs/Ge cell. Data from these cells is presented in Table 2. These measurements and comparisons indicate that the 1993 calibration values are consistent with those of previous years.

6. CONCLUSIONS

The 1993 balloon flight was a success. Nine cells from previous flights were reflown this year. Of these nine, six are Si cells and three are GaAs cells. Considering only the

Si cells, the maximum deviation of the 1993 data from the average data was -0.37% (averages were computed including the 1993 data). For the GaAs cells, the maximum deviation of the 1993 data from the average was -1.13%. These results and comparisons are similar to those achieved in previous flights, and we believe that the calibration values obtained from the 1993 flight can be used with a high degree of confidence.

7. REFERENCES

1. B. E. Anspaugh, R. G. Downing, and L. B. Sidwell, *Solar Cell Calibration Facility Validation of Balloon Flight Data: A Comparison of Shuttle and Balloon Flight Results*, JPL Publication 85-78, Jet Propulsion Laboratory, Pasadena, California, October 15, 1985.
2. *The Astronomical Almanac for the Year 1993*, U.S. Nautical Almanac Office, U.S. Naval Observatory, Superintendent of Documents, U.S. Government Printing Office, Washington, D.C. 20402, p. C12.

Table 1. 1993 Balloon Flight 7/29/93 120,000 ft, RV = 1.0152078, Flight No. 1530P

| MODULE CALIBRATION DATA | | | | COMPARISON - SOLAR SIMULATOR & FLIGHT | | | | GENERAL INFORMATION | |
|-------------------------|----------|---------------------------------|-----------|---|-------|----------------------------------|-------------------------------|---------------------|---------------------------|
| MODULE NUMBER | ORG. | TEMP INTENSITY ADJUSTED AVERAGE | STD. DEV. | AMO, SOLAR SIM. 1 AU 28 DEG C. PRE-FLT POST-FLT | | PRE-FLT. VS. POST-FLT. (PERCENT) | FLIGHT VS. PRE-FLT. (PERCENT) | TEMP. COEFF. (MV/C) | COMMENTS |
| 93-116 | GE/MM | 79.63 | 0.1345 | 79.43 | 79.14 | -0.37 | 0.19 | 0.0500 | BSR 2 Ohm |
| 93-173 | GE/MM | 82.48 | 0.0546 | 82.78 | 82.78 | 0.00 | -0.44 | 0.0464 | BSF 10 Ohm 3 mil |
| 93-174 | GE/MM | 79.56 | 0.0585 | 79.39 | 78.85 | -0.68 | 0.20 | 0.0509 | BSR 2 Ohm |
| 93-141 | HUGHES | 75.01 | 0.0452 | 75.02 | 74.99 | -0.04 | 0.11 | 0.0343 | BSFR |
| 93-143 | HUGHES | 69.13 | 0.0466 | 68.50 | 68.44 | -0.09 | 0.89 | 0.0384 | BSR |
| 93-145 | HUGHES | 83.28 | 0.1568 | 81.33 | 81.54 | 0.26 | 2.11 | 0.1377 | BSR Irradiated |
| 73-182 | JPL | 67.71 | 0.1024 | 68.05 | 68.24 | 0.28 | -0.54 | 0.0536 | HEK 2 Ohm 14 mil |
| 80-004 | JPL | 78.02 | 0.0605 | 77.99 | 77.99 | 0.00 | -0.13 | 0.0467 | K4 3/4 10 Ohm 10 mil |
| 81-004 | JPL | 77.24 | 0.1288 | 76.74 | 76.74 | 0.00 | 0.50 | 0.0455 | SPL K4 3/4 10 Ohm 10 mil |
| 84-002 | JPL | 59.06 | 0.1406 | 55.74 | 56.20 | 0.83 | 5.68 | 0.0615 | HRL GaAs |
| 86-024 | JPL | 59.01 | 0.0985 | 54.62 | 55.11 | 0.90 | 7.76 | 0.0575 | GaAs Mantech T4 |
| 86-025 | JPL | 87.49 | 0.1401 | 87.48 | 87.73 | 0.29 | 0.00 | 0.0474 | K6 3/4 8 mil T2 |
| 86-026 | JPL | 76.03 | 0.0994 | 76.02 | 75.98 | -0.05 | 0.00 | 0.0427 | K6 3/4 10 Ohm 8 mil |
| 92-001 | JPL | 61.86 | 0.1563 | 50.17 | 49.72 | -0.90 | 22.76 | -0.0447 | K6 3/4 405 nm Bandpass |
| 92-002 | JPL | 73.41 | 0.1159 | 72.22 | 71.99 | -0.32 | 1.37 | -0.0286 | K6 3/4 486 nm Bandpass |
| 92-003 | JPL | 76.99 | 0.1103 | 68.90 | 69.01 | 0.16 | 11.44 | -0.0325 | K6 3/4 577 nm Bandpass |
| 92-004 | JPL | 79.92 | 0.0788 | 70.36 | 70.43 | 0.10 | 13.38 | -0.0345 | K6 3/4 656 nm Bandpass |
| 92-005 | JPL | 60.98 | 0.1820 | 57.81 | 57.68 | -0.22 | 4.99 | 0.0589 | ASEC GaAs/Ge T1 |
| 93-001 | JPL | 60.31 | 0.1477 | 57.35 | 57.42 | 0.12 | 4.91 | 0.0654 | SPL GaAs/Ge |
| 93-002 | JPL | 79.47 | 0.0591 | 80.13 | 80.13 | 0.00 | -0.75 | 0.0460 | ASEC 10 Ohm 4 mil |
| 93-003 | JPL | 81.00 | 0.1005 | 80.99 | 80.86 | -0.16 | -0.23 | 0.0602 | ASEC 10 Ohm 8 mil |
| 93-004 | JPL | 80.69 | 0.1225 | 80.46 | 80.55 | 0.11 | 0.17 | 0.0577 | ASEC 10 Ohm 8 mil |
| 93-005 | JPL | 55.13 | 0.1208 | 47.54 | 47.52 | -0.04 | 15.80 | -0.0430 | K6 3/4 400 nm Bandpass |
| 93-006 | JPL | 74.67 | 0.1308 | 65.47 | 65.41 | -0.09 | 13.67 | -0.0417 | K6 3/4 500 nm Bandpass |
| 93-007 | JPL | 63.93 | 0.1013 | 57.50 | 57.56 | 0.10 | 10.90 | -0.0172 | K6 3/4 600 nm Bandpass |
| 93-008 | JPL | 65.71 | 0.1612 | 57.34 | 57.05 | -0.51 | 14.14 | -0.0713 | K6 3/4 700 nm Bandpass |
| 93-009 | JPL | 65.21 | 0.0399 | 42.49 | 43.18 | 1.62 | 53.36 | -0.0237 | K6 3/4 800 nm Bandpass |
| 93-010 | JPL | 56.40 | 0.1508 | 83.90 | 85.53 | 1.94 | -32.53 | -0.1472 | K6 3/4 900 nm Bandpass |
| 93-011 | JPL | 61.62 | 0.0805 | 55.57 | 55.44 | -0.23 | 10.75 | 0.0351 | K6 3/4 1000 nm Bandpass |
| STS-021 | JPL | 73.14 | 0.0589 | 72.49 | 72.94 | 0.62 | 0.80 | 0.0543 | K4 3/4 High Blue Resp. T3 |
| 93-154 | MM | 20.63 | 0.3896 | 27.01 | 21.68 | -19.73 | -25.60 | 0.0532 | CdTe |
| 93-162 | MSFC | 64.34 | 0.1000 | 60.81 | 60.91 | 0.16 | 5.48 | 0.0621 | ASEC GaAs/Ge |
| 93-163 | MSFC | 76.70 | 0.0911 | 77.18 | 76.82 | -0.47 | -0.67 | 0.0417 | SPL K6.7 3.5 mil |
| 93-132 | SANDIA | 84.21 | 0.1083 | 85.78 | 84.08 | -1.98 | -1.98 | 0.0633 | Sandia Si Cell |
| 93-122 | SS-LORAL | 61.43 | 0.1171 | 58.16 | 58.25 | 0.15 | 5.25 | 0.0647 | GaAs/Ge |
| 92-131 | TRW | 32.78 | 0.0425 | 29.98 | 29.90 | -0.27 | 9.21 | 0.0346 | Amorphous Si |
| 93-102 | TRW | 60.30 | 0.0948 | 57.00 | 56.89 | -0.19 | 5.54 | 0.0605 | GaAs/Ge 5.5 mil |
| 93-103 | TRW | 80.98 | 0.0743 | 80.76 | 80.76 | 0.00 | 0.24 | 0.0556 | BSR 8 mil |
| 93-105 | TRW | 81.84 | 0.1140 | 81.61 | 81.50 | -0.13 | 0.23 | 0.0545 | BSR 8 mil |
| 93-107 | TRW | 61.65 | 0.1054 | 58.05 | 58.29 | 0.41 | 5.90 | 0.0526 | GaAs/Ge FAST |
| 0 mV | | 0.00 | 0.0000 | | | | | | |
| 50 mV | | 50.01 | 0.0561 | | | | | | |
| 80 mV | | 80.05 | 0.0383 | | | | | | |
| 100 mV | | 99.88 | 0.1400 | | | | | | |

Table 2. Repeatability of Nine Standard Solar Cell Modules Over a 20-year Period

| Flight Date | 73-182 HEK | 80-004 K 4 3/4 BSR | 81-004 K 4 3/4 BSR | 84-002 HRL GaAs | STS-021 High Blue | 86-024 GaAs Man- Tech | 86-025 K 6 3/4 | 86-026 K4 3/4 | 92-005 GaAs/Ge |
|----------------|---------------|--------------------------|--------------------------|-----------------------|-------------------------|--------------------------------|-------------------|------------------|-------------------|
| 4/5/74 | 68.37 | | | | | | | | |
| 6/6/75 | 67.88 | | | | | | | | |
| 6/10/77 | 67.96 | | | | | | | | |
| 7/20/78 | 68.20 | | | | | | | | |
| 8/8/79 | 67.83 | | | | | | | | |
| 7/24/80 | 68.00 | 78.06 | | | | | | | |
| 7/25/81 | 67.96 | | 77.55 | | | | | | |
| 7/21/82 | 68.03 | 78.05 | 77.52 | | | | | | |
| 7/12/83 | 68.03 | | | | | | | | |
| 7/19/84 | 67.62 | | | 59.61 | | | | | |
| 8/84 Shuttle | | | | | 73.60 | | | | |
| 7/12/85 | | | | | 72.85 | | | | |
| 7/15/86 | | | | | | 58.44 | 87.71 | 76.25 | |
| 8/23/87 | | | | 59.77 | | 59.59 | 87.99 | | |
| 8/7/88 | | | 77.49 | | | 58.36 | 87.00 | | |
| 8/9/89 | | | | | | | | | |
| 9/6/90 | | 78.33 | 77.43 | 59.46 | | 58.84 | 87.77 | | |
| 8/1/91 | | 77.98 | | | | 58.89 | 87.34 | | |
| 8/1/92 | | | | | 73.08 | | | 76.29 | 62.31 |
| 7/29/93 | 67.71 | 78.02 | 77.28 | 59.06 | 73.14 | 59.01 | 87.49 | 76.03 | 60.92 |
| Average | 67.963 | 78.088 | 77.454 | 59.475 | 73.168 | 58.855 | 87.550 | 76.190 | 61.615 |
| Std. Deviation | 0.209 | 0.139 | 0.107 | 0.304 | 0.314 | 0.443 | 0.352 | 0.140 | 0.983 |
| Max. Deviation | 0.407 | 0.242 | 0.174 | 0.415 | 0.433 | 0.735 | 0.550 | 0.160 | 0.695 |

